

## Investigation of Initial Voltage Distributions in HV Windings of Shunt Reactors Taking Voltage Impulses into Account

### Khảo sát sự phân bố điện áp ban đầu trong cuộn dây cao áp của cuộn kháng bù ngang có xét đến ảnh hưởng các xung điện áp

Hung Bui Duc\*, Trinh Cong Truong, Tu Pham Minh, Dinh Bui Minh and Vuong Dang Quoc

School of Electrical and Electronic Engineering, Hanoi University of Science and Technology

\*Corresponding author: [hung.buiduc@hust.edu.vn](mailto:hung.buiduc@hust.edu.vn)

#### Abstract

Shunt reactors operating in high and super voltage systems are usually influenced by voltage impulses that cause transient over voltages. Many authors have been recently studied influence of fringing fluxes around air gaps, leakage inductances and the number of air gaps to the shunt reactors. In this paper, an analytic technique is proposed to investigate and analyse initial voltage distributions with different types of high voltage shunt reactor's winding when affected by a lightning impulse/voltage impulse. In order to make the uniformly distribution in the winding, it is necessary to change the winding type by increasing series capacitance values. Thus, the model of shunt reactor's winding will be proposed via an analytic method to compute capacitance components in the windings. The obtained results from the analytic method are then introduced to the ATPDraw tool to simulate and investigate the initial voltage distributions in high voltage windings.

**Key words:** Shunt reactors, high voltage winding types, initial voltage distribution, analytic method, ATPDraw tools.

#### Tóm tắt

Các cuộn kháng bù ngang vận hành trong hệ thống điện cao áp và siêu cao áp thường bị ảnh hưởng bởi các xung điện áp và là nguyên nhân gây ra hiện tượng quá độ điện áp. Nhiều tác giả gần đây đã nghiên cứu sự ảnh hưởng của từ thông tản xung quanh khe hở không khí, điện cảm rò và số lượng khe hở không khí trong mạch từ của cuộn kháng. Trong bài báo này, phương pháp giải tích được đề xuất để khảo sát và phân tích sự phân bố điện áp ban đầu với các kiểu dây cao áp khác nhau của cuộn kháng khi bị ảnh hưởng bởi xung sét/xung điện áp. Để cho sự phân bố điện áp trong cuộn dây được đồng đều, việc thay đổi kiểu quấn dây bằng cách tăng các giá trị tụ điện nối tiếp là rất cần thiết. Bởi vậy, mô hình dây quấn cuộn kháng được đề xuất thông qua phương pháp giải tích để tính toán các thành phần của giá trị tụ điện trong dây quấn. Các kết quả đạt được từ mô hình giải tích sẽ được tích hợp vào phần mềm "ATPDraw tool" để mô phỏng và khảo sát sự phân bố ban đầu của dây cao áp.

**Từ khóa:** Cuộn kháng điện, kiểu dây quấn cao áp, sự phân bố điện áp ban đầu, phương pháp giải tích, ATPDraw tool.

#### 1. Introduction

Many papers have been recently investigated and studied high voltage shunt reactors (HVSRSs), that is, in [1], authors have analyzed basic parameters to the iron core of HVSRSs. In [2], the influence of fringing fluxes around air gaps, leakage inductances and the number of air gaps has been presented. However, the voltage distribution in windings of the HVSRSs

has been still not considered so far, even the problem of initial voltage distributions in the windings has been proposed for many years [3], where the transient voltage distribution is highly non uniform. In addition, it can be seen that there are 60% of these voltages appearing across 10% length of the winding [4]. This means that the insulation of the conductors can be damaged by the non-uniform voltage distribution.

Many solutions are proposed for manufacturing technology to improve the initial voltage distributions by changing the winding type [5]-[9]. With the structural similarity, the shunt reactor winding considering as the high voltage winding of a transformer is considered. In general, the transformer winding may be represented as a complex network of resistive, inductive, capacitive elements being an equivalent disks, layers and turns. All these electrical elements can be calculated via the analytic method. This equivalent circuit model has been trusted by many authors. Because the inductances have no effect on the initial voltage distributions since the magnetic field requires a finite time to build up, thus the inductances practically do not carry any current, and the voltage distribution is predominantly decided by the capacitance in the network [10]-[13]. A distribution constant  $\alpha = \sqrt{C_g/C_s}$  ( $C_g$  is the total ground capacitance and  $C_s$  is the series capacitance respectively) is used to denote the voltage distribution quality. It should be noted that the smaller value of  $\alpha$ , the more uniform the initial voltage distribution. When the winding type is changed, then the values of  $\alpha$  and capacitance are changed. In practical manufacturing, the interleaved winding is used as one of the ways to linearize the initial voltage distributions.

The ATPDraw tool is an open-source code that allows to extend the code and to calculate the values of the power system in the time domain. The differential equations of voltage and current at any point are solved by converting them in the time domain into algebraic equations by suitable transformation.

In this paper, an analytic method is presented to compute the capacitance values of high voltage windings. Then, an equivalent model is introduced to the ATPDraw tool [13], to validate and simulate obtained results from the analytic method. The comparison of initial voltage distributions between winding types (continuous disk winding, interleaved turns) on each pair of disk winding will be presented. The interleaved winding type I and the interleaved each disk on each pair of disk winding (interleaved winding type II) are pointed out in Figure 1 [11].

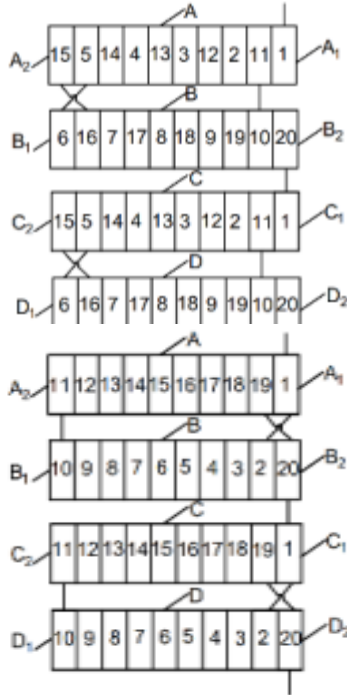


Figure 1. Interleaved winding type I (top) and type II (bottom) [11].

## 2. Analytic model of SR windings

In order to simulate the initial voltage distributions in the SR winding, it is necessary to know the winding parameters. The basic parameters of SR is given in Table 1 [2].

The simplified equivalent model for shunt reactor winding is shown in Figure 2. The capacitance between the winding and tank is computed as:

$$C_{g1} = \frac{2\pi\epsilon_0 H}{\cosh^{-1}\left(\frac{S}{R}\right)} \left( \frac{t_{oil} + t_{solid}}{\epsilon_{oil} + \epsilon_{solid}} \right), \quad (1)$$

where  $H$  is the height of conductor,  $s$  is the distance of the winding axis from the plane,  $R$  is the radius of the winding,  $t_{oil}$  and  $t_{solid}$  are the thickness of oil and solid insulations.

The capacitance between the winding and core is defined as:

$$C_{g2} = \frac{\epsilon_0 \pi D_m H}{\frac{t_{oil}}{\epsilon_{oil}} + \frac{t_{solid}}{\epsilon_{solid}}}, \quad (2)$$

where  $D_m$  is the mean diameter of the winding.

The turn-to-turn capacitance is given as:

$$C_T = \frac{\epsilon_o \epsilon_p \pi D_m (w + t_p)}{t_p}, \quad (3)$$

where  $w$  is the bare width of conductor in axial direction and  $t_p$  is the thickness of total paper insulations. The total axial capacitance between two consecutive disks based on geometrical considerations only is given by:

$$C_D = \epsilon_0 \left[ \frac{k}{\frac{t_p}{\epsilon_p} + \frac{t_s}{\epsilon_{oil}}} + \frac{1-k}{\frac{t_p}{\epsilon_p} + \frac{t_s}{\epsilon_s}} \right] \cdot \pi \cdot D_m (W_w + t_s), \quad (4)$$

where  $W_w$  is the width of the winding and  $k$  is fraction of circumferential space occupied by the oil.

The series capacitance of continuous disk winding is given as:

$$C_S = \frac{C_T}{2n^2} (n-1) + \frac{C_D}{3} \quad (5)$$

where  $n$  is the number of turns in a disk.

The series capacitances of interleaved winding type I and II are then expressed as:

$$C_{S(I)} = \frac{C_T}{4} (n-1) + \frac{C_D}{3}, \quad (6)$$

$$C_{S(II)} = \frac{C_T}{2n} (2n-3) + \frac{C_D}{3}. \quad (7)$$

Table 1: Test shunt reactor data [2].

Rating	50 MVAR
Voltage	500 kV
Frequency	50 Hz
Diameter of iron core	591 mm
Height of winding	1343 mm
Width of winding	203 mm
Number of turns	2925
Cross-section of conductor	20,25 mm <sup>2</sup>
Turn-to-turn insulation	Paper
Winding-to-core insulation	Oil

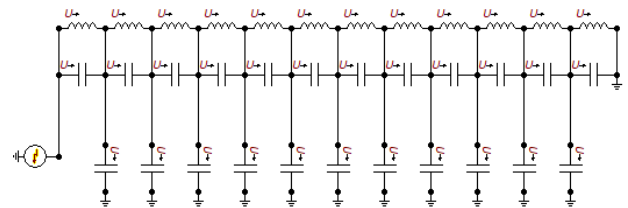


Figure 2. Simplified equivalent model for shunt reactor winding.

## 3. Application test

Based on the theory developed in the previous part, the computed values are introduced to ATPDraw tools [13] to compute and simulate the practical problem. There are two cases considered in this research, that is:

- **Case 1:** The winding with 61 disks is considered. The first three disks consist of 47 turns for each disk, and 48 turns for each disk for the rest of the winding. The total thickness of paper insulation is 0,5 mm. The lightning impulse 1,2/50 following to IEC standard is applied. When the neutral is grounded, the results of voltage distribution with different

types of windings at disk 1<sup>st</sup>, 10<sup>th</sup>, 28<sup>th</sup>, 37<sup>th</sup>, 46<sup>th</sup>, 55<sup>th</sup>, 60<sup>th</sup> are shown below Figures (from Figure 3 to Figure 5).

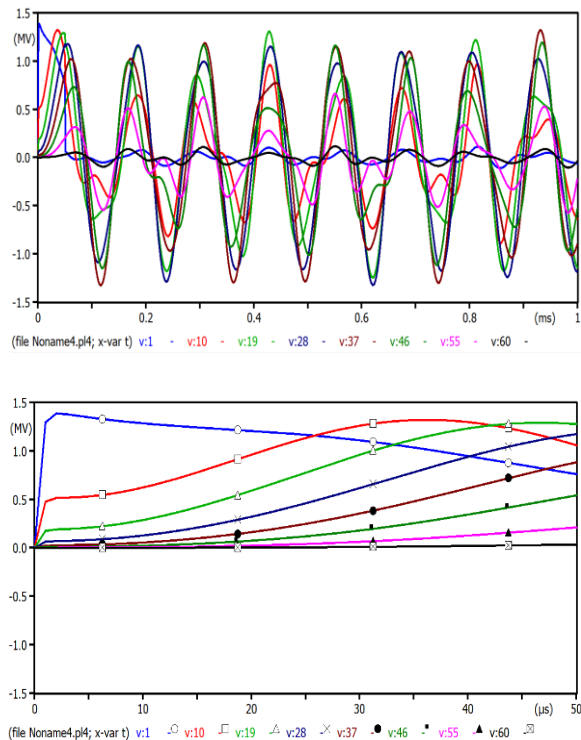


Figure 3. Continuous disk winding (case 1).

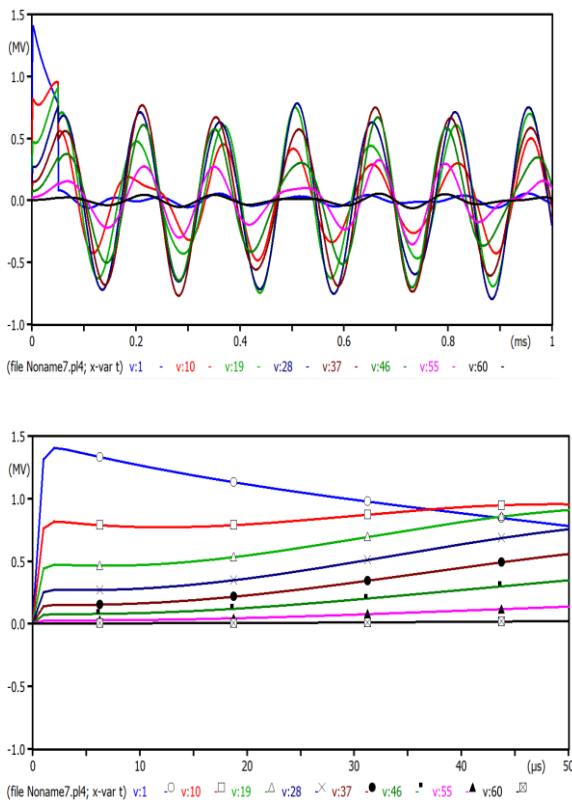


Figure 4. Interleaved winding type I (case 1).

In Figure 3, the different voltage between the 1<sup>st</sup> disk and the 10<sup>th</sup> disk is 947,71 kV, while the different voltage between

the 10<sup>th</sup> disk and 19<sup>th</sup> is obtained 316,69 kV. In other words, the first 10 disks carry 60% of the voltage drop in the winding.

In Figure 4, it can be shown that the different voltage between the 1<sup>st</sup> disk and the 10<sup>th</sup> disk reaches to 681,04 kV. Or it means that the first 10 disks carry 43,93% of the voltage drop in the winding, which has improved in comparison with the continuous disk windings.

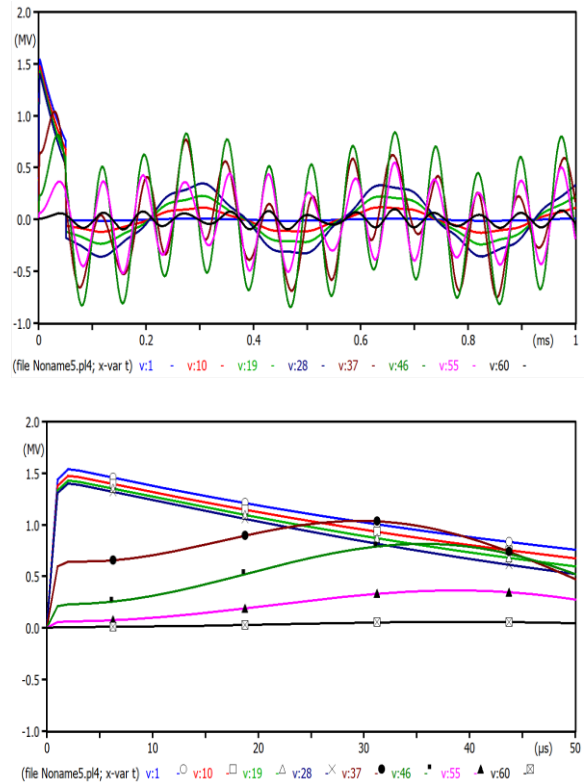


Figure 5. Interleaved winding type II (case 1).

In Figure 5, the voltage difference between the 1<sup>st</sup> disk and the 10<sup>th</sup> disk is just 260,9 kV, while the different voltage between the 10<sup>th</sup> disk and 19<sup>th</sup> is 244,8 kV. Therefore, for this winding type, the voltage distribution across the winding becomes much more uniform.

Finally, the waveforms of initial voltage distributions at 2μs for different types of windings are pointed out in Figure 6. There are big changes of voltage distribution for the interleaved winding I and continuous disk winding. The voltage is very high at first disks and is reduced at the end disks.

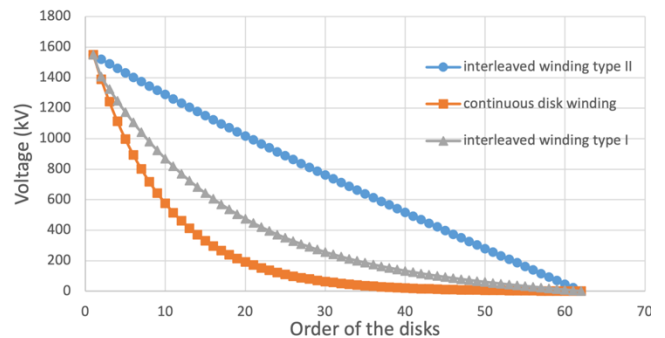


Figure 6. Initial voltage distributions (case 1).

- **Case 2:** As mentioned above, the first disks are subjected to the large voltage. In this case, the first 8 disks are reinforced insulation.

have 48 turns in each disks. Thus, the winding has total 63 disks. The lightning impulse 1,2/50 is applied again, notice that the neutral is grounded and the simulation results of voltage distribution at disk 1<sup>st</sup>, 10<sup>th</sup>, 19<sup>th</sup>, 28<sup>th</sup>, 37<sup>th</sup>, 46<sup>th</sup>, 55<sup>th</sup>, 62<sup>nd</sup> are shown from Figure 7 to Figure 9.

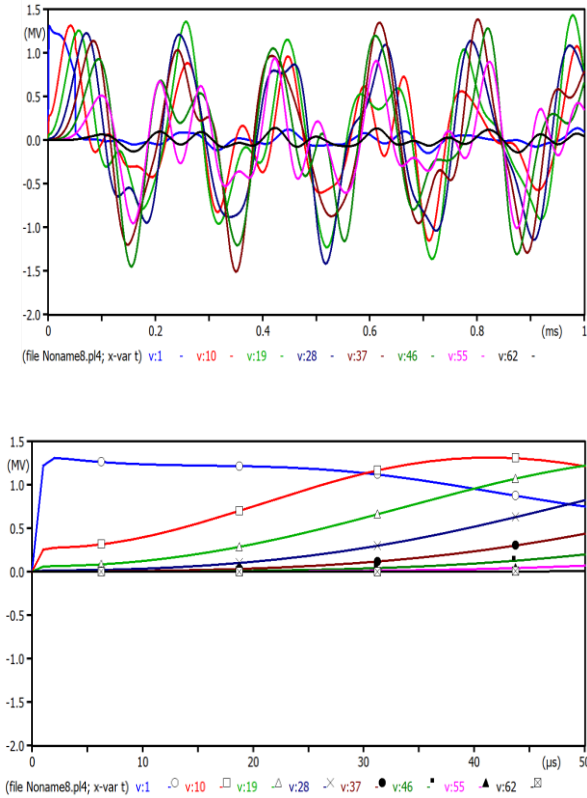


Figure 7. Continuous disk winding (case 2).

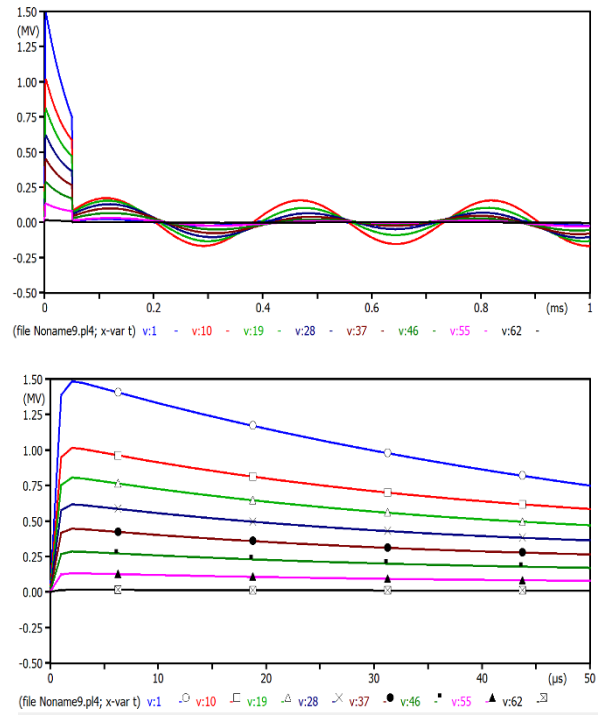


Figure 9. Interleaved winding type II (case 2).

In Figure 7, the voltage difference between the 1<sup>st</sup> disk and the 10<sup>th</sup> disk is up to 1222,49 kV, while the voltage difference between the 10<sup>th</sup> disk and 19<sup>th</sup> is just 253,857 kV. In other words, the first 10 disks carry 78,87% of the voltage drop on the winding. In Figure 8, the voltage difference between the 1<sup>st</sup> disk and the 10<sup>th</sup> disk is 965,79 kV. It means that the first 10 disks carry 62,3% of the voltage drop in the winding, which is still not good for the winding.

In Figure 9, the voltage difference between the 1<sup>st</sup> disk and the 10<sup>th</sup> disk is 508,9 kV. In fact, this voltage drop is not large enough to destroy the conductor insulation. It should be noted that that this type of winding will help to make the voltage distribution become more uniform.

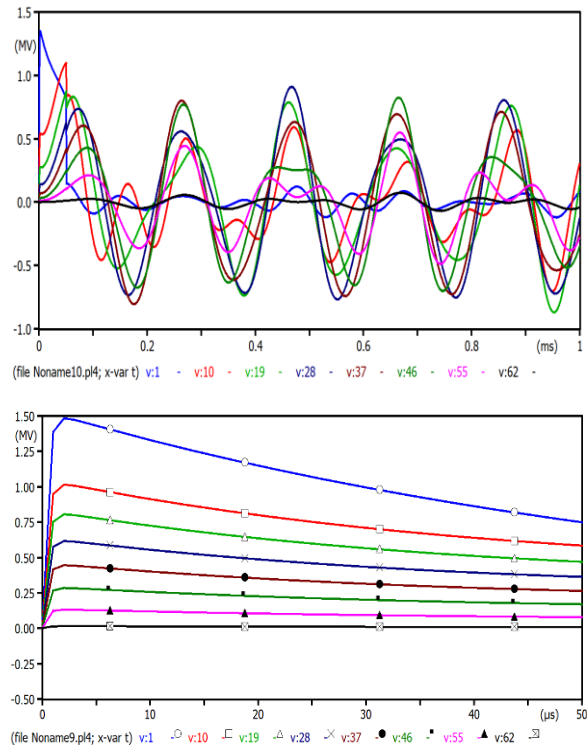


Figure 8. Interleaved winding type I (case 2).

The total paper insulation thickness of conductor in these disks is 1,5 mm. Each disk of these 8 disks has 38 turns. The next 19 disks have 47 turns in each disk. And the last 36 disks

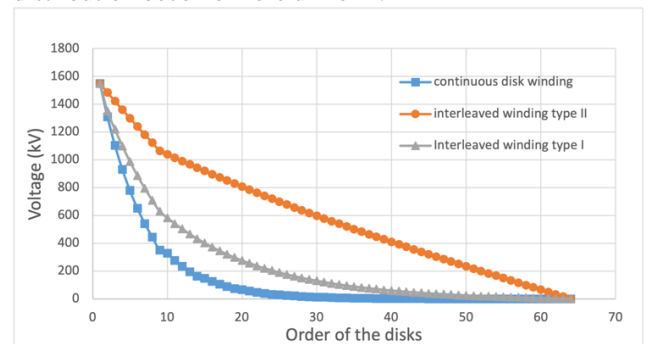


Figure 10. Initial voltage distributions (case 2).

Figure 10 finally shows the waveforms of initial voltage distributions at 2μs for different types of windings.

In the same way to the results obtained from Figure 6, the voltage distribution for the interleaved winding I and

continuous disk winding are very large at the first disks and are reduced at the end disks.

DATA	UNIT	VALUE	NODE	PHASE	NAME
C	μF	0.01084	From	1	
Ks	Damp 0.1-0.2	0	To	1	

DATA	UNIT	VALUE	NODE	PHASE	NAME
C	μF	7.423E-6	From	1	
Ks	Damp 0.1-0.2	0	To	1	

**Figure 11.** Series capacitance (top) and parallel capacitance (bottom).

The value of series and parallel capacitances are also shown via the interface screen simulated by ATPDraw tools [13] as presented in Figure 11. Where the series capacitance value is  $0.01084 \mu F$  and  $7.423 \cdot 10^{-6}$  for the parallel capacitance value.

## 4. Conclusions

In this paper, the initial voltage distribution of different SR winding types has been successfully analysed and investigated by the analytic model and ATPDraw tools [13]. The study has shown that instead of using continuous disk winding with large voltage stress drop across the first disks, the interleaved winding types help to improve the initial voltage distribution across the disks. It can be seen that the distribution line is more linearized with the interleaved winding types. It should be noted that the obtained results of this paper can help researchers and manufacturers to define and make a suitable selection for the type of a SR winding in practice.

## References

- [1] Tu Pham Minh, Hung Bui Duc, Thanh Tran Van, Vuong Dang Quoc. Investigating Effects of Distance Air-Gaps on Iron-Core Shunt Reactors. Lecture Notes in Networks and Systems; ISBN 978-3-030 92573-4, (Scopus, Q4, H-index 22), pp.543-557. [https://link.springer.com/chapter/10.1007/978-3-030-92574-1\\_57](https://link.springer.com/chapter/10.1007/978-3-030-92574-1_57), 2021.
- [2] T. P. Minh, "Finite Element Modeling of Shunt Reactors Used in High Voltage Power Systems", *Eng. Technol. Appl. Sci. Res.*, vol. 11, no. 4, pp. 7411–7416, Aug. 2021.
- [3] Kanchan Rani, R. S. Gorayan, "Very Fast Transient Overvoltages in Transformer (EMTP Simulation and Experimental Studies)", Conference paper, ResearchGate, February, 2013.
- [4] Gao Youhua, Yuan Hong, Wang Erazi, and Cao Yundong, "Calculation Of Very Fast Transients Over-Voltage And Its Distribution In Transformer Winding In 110 kV GIS", Seoul Korea: proceeding of international conference on electrical machines and systems, 2007, oct 8–11.
- [5] M. Popov, L. Sluis, R. P. P. Smeets, J. L. Rolda, "Analysis of very fast transients in layer-type transformer windings", *IEEE Trans. on Pow. Deliv.*, vol. 22, no. 1, pp. 238 - 247, Jan. 2007.
- [6] L. Satish, A. Jain, "Structure of transfer function of transformers with special reference to interleaved windings", *IEEE Trans. on Pow. Deliv.*, vol. 17, pp. 754 - 760, 2002.
- [7] M. Florkowski, J. Furga, "Detection of transformers winding deformation based on transfer function - measurement and simulations", *Meas. Scien and Techn.*, no. 14, pp. 1986 - 1992, 2003.

- [8] M. Florkowski, J. Furga, "Transformer winding defects identification based on high frequency method", *Measur. Scien. and Techn.*, no. 18 pp. 28272 - 835, 2007.
- [9] J. Mikulović, M. Savić, "Calculation of transients in transformer winding and determination of winding parameters", *Electr. Engin.*, no.89, pp. 293-300., 2007.
- [10] . Lucas, H.H. Narsinga Rao & K. Bheema Prakash, "GIS Fast transients – investigation of surge propagation within transformer winding", Third workshop conference on EHV technology, IISC Bangalore, p.p. 79-83, Aug 1995.
- [11] Marek Florkowski, Jakub Furgał, "Initial voltage distributions in transformer windings at ultra-fast stresses", *IEEE*, Polish Ministry of Science and Higher Education, 2010.
- [12] S.V.Kulkarni, S.A.Khaparde, "Transformer Engineering, Design and Practice", Marcel Dekker, Inc, 2005.
- [13] Bienvenido R.-M. ,Mariana Santiago-Luna, "EMTP/ATP Quick Guide Electric Power Engineering Group - UPR", Mayagüez. PR., 2002

## Author's Biography



**Dr. Bui Duc Hung** is currently working as a team leader of electrical machines's group, and also a lecturer of Department of Electrical Engineering, School of Electrical Engineering, Hanoi University of Science and Technology. He obtained the PhD degree in the Department of Electrical Engineering, Hanoi University of Science and Technology, in 2000.



**Engineer Trinh Cong Truong** is currently a master student at the Department of Electrical Engineering, School of Electrical and Electronic Engineering, Hanoi University of Science and Technology. He obtained the Engineer degree in the Department of Electrical Engineering, Hanoi University of Science and Technology, in 2021.



**Dr. Bui Minh Dinh** is currently working as a lecturer at the Department of Electrical Engineering, School of Electrical and Electronic Engineering, Hanoi University of Science and Technology. He obtained the PhD degree in the Department of Electrical Engineering, TU university, in 2014.



**Dr. Pham Minh Tu** is currently working as a lecturer at the Department of Electrical Engineering, School of Electrical Engineering, Hanoi University of Science and Technology. He obtained the PhD degree in the Department of Electrical Engineering, Hanoi University of Science and Technology, in 2021.



**Assoc. Prof. Dang Quoc Vuong** is currently a deputy director of Training Center of Electrical and Electronic Engineering, and also a lecturer of Department of Electrical Engineering, School of Electrical Engineering, Hanoi University of Science and Technology. He obtained the PhD degree in the Electrical Engineering and Computer Science Department of the University of Liège, Belgium, in 2013.